Available online at www.sciencedirect.com

ScienceDirect

IFAC PapersOnline CONFERENCE PAPER ARCHIVE

IFAC PapersOnLine 51-28 (2018) 720–725

Deep Koopman Controller Synthesis for Cyber-Resilient Market-Based Frequency Regulation

Pengcheng You * **John Pang** ** **Enoch Yeung** ***

* *Zhejiang University, Hangzhou, China (e-mail: pcyou@zju.edu.cn).*
** *Caltech, Pasadena, CA, USA (e-mail: jzpang@caltech.edu)*
*** *Pacific Northwest National Laboratory, Richland, WA, USA (e-mail: enoch.yeung@pnnl.gov)*

Abstract: This paper investigates a data-driven countermeasure for price spoofing in the context of cyber security and market-based frequency regulation. Market-based control of transmission power networks relies on cyber-physical infrastructure, which raises questions of system vulnerability in relation to cyber-security. In this paper, we consider the challenge of engineering a robust data-driven controller in the presence of price spoofing, i.e. where hacking mechanisms adjust price signals in an ex-post market. We extend a recently developed algorithm called deep dynamic mode decomposition to learn Koopman operators of nonlinear systems with affine inputs. Based on the learned input-Koopman operator model, a design algorithm for nonlinear controller synthesis is devised to compute optimal dynamic pricing policies that restore the nominal frequency and recover economic efficiency in the presence of price spoofing. The efficacy of the proposed data-driven Koopman controller synthesis approach is validated through tests on a IEEE 39-bus benchmark.

Keywords: Market-based frequency regulation, input-Koopman operator, data-driven controller synthesis, dynamic feedback control, cyber-security, price spoofing

1. INTRODUCTION

An ideal power system operates at a nominal frequency, e.g., 60 Hz in the US, where power generation and consumption are balanced over the whole network. Any instant imbalance drives frequency away from its nominal value, causing operational efficiency loss, and if left unattended, collapses the system if the deviation exceed security limits. Frequency regulation has always been one of the most fundamental problems in power system operation, which takes joint steps to maintain the nominal frequency across different timescales. It consists of three stages: (1) primary - frequency stabilization within low tens of seconds; (2) secondary - frequency restoration in up to two or three minutes; (3) tertiary - economic dispatch at the timescale of minutes or up.

The state of the art for frequency regulation in industrial practices includes droop control at the primary stage and automatic generation control (AGC) at the secondary stage. Recently there has been significant interest in viewing the problem from a reverse-engineering perspective. Zhao et al. (2016) proposes a primary control design that carries out a variant primal-dual gradient algorithm to solve an underlying economic dispatch problem and also shows that droop control is just one specific case of this controller. Li et al. (2016) adopts a similar approach to demonstrate the economic inefficiency of AGC to restore frequency and thereafter develops an alternative optimal decentralized controller in terms of equilibrium economic dispatch. In addition, due to the volatility of emerging renewable generation, increasing work, e.g., Zhao et al. (2014); Pang et al. (2017); Mallada et al. (2017), takes into account load-side control for frequency regulation to complement the traditional generation-side efforts.

As aforementioned, the economic concerns of frequency regulation have arisen and drawn much attention. One natural approach to guarantee economic efficiency without central governance is to resort to a competitive market. Therefore, a significant amount of existing literature has centered around market-based frequency control. The idea of dynamical markets was first proposed by Alvarado et al. (2001) to investigate the stability of an interconnected power system coupled with market dynamics. Therein an eigenvalue analysis is applied to the linearized model. Then Stegink et al. (2016, 2017) focuses on the closed-loop system of a higher-fidelity power network model and market dynamics in the port-Hamiltonian form, which contributes to the proof of its asymptotic stability. Jokic et al. (2009) illustrates how global objectives and constraints can be optimally translated into time-varying market prices that reflect the state of physical systems as well as guide and coordinate generations and loads. You et al. (2018) follows the reverse-engineering approach to design a more explicit dynamical market model and proves the asymptotic stability of linearized swing dynamics coupled with the proposed market dynamics. Liang et al. (2015) looks at the hybrid dynamics that couple power systems with power markets in a more realistic discrete-time model and also demonstrates the corresponding asymptotic stability.

10.1016/j.ifacol.2018.11.790

The theory for market-based frequency control has been flourishing in the past decade. Most, if not all, existing works address the problem from the canonical model-driven point of view, which proves to function well under normal conditions. However, nowadays key infrastructure like a power network is readily exposed to cyber-security threat. Cyber-attacks invade vulnerable parts of cyber-physical systems to disrupt their normal operation. Power markets, as a natural cyber-layer of power systems to release price signals, are easily infectable subject to spoofing, manipulation, false data injection, etc. Due to unknown characterization of cyber-attacks, most model-driven methods for frequency control will fail to function. It is thus imperative to have a robust control design that is resilient and invulnerable to such cyber-attacks.

This work focuses on a power network with its generators and loads rationally responsive in an *ex-post* power market, which functions as a controller to maintain the nominal frequency. We consider the case where any pricing strategy to clear the market is subject to unknown spoofing at the cyber-layer that intends to either destabilize the system or perturb the equilibrium economic dispatch. Our goal is to devise a price controller that is robust against spoofing and recovers economic efficiency.

To this end, a deep input-Koopman learning method is used to characterize the nonlinear suite of dynamics comprised of open-loop swing dynamics, market participants' behavior and an unknown price spoofing mechanism. A deep neural network is adopted to learn from real-time data the set of basis functions of the space (dictionary) and the corresponding linear law (the Koopman operator). With the learned linear Koopman model, we propose a controller synthesis problem to determine a pricing strategy that is able to restore the nominal frequency and recover the efficiency of economic dispatch. More importantly, this data-driven controller design can adaptively capture an unknown price spoofing mechanism and is thus resilient to cyber-attacks, robustly achieving secondary frequency control.

2. MARKET-BASED FREQUENCY CONTROL

Let $\mathbb{R}$ ($\mathbb{R}_+$ and $\mathbb{R}_-$) be the set of (positive and negative) real numbers and $\mathbb{N}$ be the set of natural numbers. For a finite set $\mathcal{H} \subset \mathbb{N}$, its cardinality is denoted as $|\mathcal{H}|$. For a set of scalar variables y_j, $j \in \mathcal{H}$, its column vector is denoted as $y_{\mathcal{H}}$. The subscript $\mathcal{H}$ may be dropped if the set is clear from the context. For a matrix Y, Y^T denotes its transpose. Let Y_j be the jth row of Y and $Y_{\mathcal{H}}$ be submatrix of Y composed of all the rows Y_j, $j \in \mathcal{H}$. We use $1_{\mathcal{H}}$ or $0_{\mathcal{H}}$ to denote a $|\mathcal{H}|$-dimension column vector of all 1's or 0's. Similarly, if the subscript $\mathcal{H}$ is clear without ambiguity, it may be ignored.

2.1 System Model

Consider a power network with a connected directed graph $(\mathcal{N}, \mathcal{E})$, where $\mathcal{N} := \{0, 1, \ldots, |\mathcal{N}| - 1\}$ is the set of nodes and $\mathcal{E} \subset \mathcal{N} \times \mathcal{N}$ is the set of edges connecting all nodes. Each node represents a bus and each edge is a transmission line. The buses are partitioned into two categories $\mathcal{N} = \mathcal{G} \cup \mathcal{L}$ where $\mathcal{G}$ and $\mathcal{L}$ are the sets of generator and load buses, respectively. Note that a generator bus could also have local loads. For notational convenience, assume each generator bus has only one (aggregate) synchronous generator and one (aggregate) load while each load bus has just one (aggregate) load. We will use (j, k) and $j \to k$ interchangeably to denote the line from bus j to bus k. An arbitrary orientation is applied such that if $(j, k) \in \mathcal{E}$ then $(k, j) \notin \mathcal{E}$. Each line $(j, k) \in \mathcal{E}$ is endowed with an impedance z_{jk}, where the real part is a resistance while the imaginary part is a reactance.

Let θ_j be the bus phase angle, ω_j be the bus frequency, p_j be the output of a generator, d_j be an elastic load and E'_{qj} be the q-axis transient internal voltage of a generator. Note that $\theta_j, \omega_j, p_j, d_j$ are all deviations from a nominal static equilibrium. Consider a nonlinear network model of swing dynamics and voltage dynamics from Wang et al. (2017); Stegink et al. (2017, 2016), alternatively reduced:

$$\dot{\theta}_j = \omega_j, \quad j \in \mathcal{G} \tag{1a}$$

$$M_j \dot{\omega}_j = p_j - d_j - D_j \omega_j - \sum_{k:j\to k} f_{jk} + \sum_{i:i\to j} f_{ij}, \quad j \in \mathcal{G} \tag{1b}$$

$$D_j \dot{\theta}_j = -d_j - \sum_{k:j\to k} f_{jk} + \sum_{i:i\to j} f_{ij}, \quad j \in \mathcal{L} \tag{1c}$$

$$T'_{dj} \dot{E}'_{qj} = E_{fj} - [1 - X_j B_{jj}] E'_{qj} + X_j \sum_{k\in\mathcal{N}(j)} l_{jk}, \quad j \in \mathcal{G} \tag{1d}$$

where $X_j := x_{dj} - x'_{dj}$, $l_{jk} := E'_{qk} B_{jk} \cos(\theta_j - \theta_k)$, $f_{jk} := E'_{qj} E'_{qk} B_{jk} \sin(\theta_j - \theta_k) - f^0_{jk}$ is the line flow deviation from its nominal value f^0_{jk}, and $\mathcal{N}(j)$ denotes the set of neighbor buses that are connected to bus j. Therein M_j is generator j's inertia, D_j is a constant factor summarizing generator damping effects, if any, and uncontrollable frequency-dependent loads. $B_{jk} := \frac{1}{x_{jk}}$ is the negative susceptance of a line, and $B_{jj} := \sum_{k\in\mathcal{N}(j)} \frac{1}{x_{jk}}$ is the self susceptance of a bus. For each generator j, T'_{dj} is the d-axis transient time constant, E_{fj} is the constant excitation voltage set to 1, and x_{dj} and x'_{dj} are the d-axis synchronous and transient reactances, respectively. Basically two standard assumptions are made to derive this model: (a) each line $(j, k) \in \mathcal{E}$ is lossless, i.e., $z_{jk} := \mathbf{i} x_{jk}$; (b) reactive loads are ignored.

In the case of instant power imbalance in a power network, a dynamical *ex-post* power market is employed to restore frequency to its nominal value instead of traditional regulation service. If well designed, the market mechanism realizes economic dispatch in nature. We assume a *competitive* market where all participants are rational and none of them able to exercise market power. Suppose all generators and loads are responsive in the *ex-post* power markets, then their rational dynamical behavior is modeled by:

$$T^v_j \dot{v}_j = -v_j + p_j + u_j - J'_j(p_j), \quad j \in \mathcal{G} \tag{2a}$$

$$T^p_j \dot{p}_j = -p_j + v_j, \quad j \in \mathcal{G} \tag{2b}$$

$$T^d_j \dot{d}_j = U'_j(d_j) - u_j, \quad j \in \mathcal{N} \tag{2c}$$

where T^v_j, T^p_j and T^d_j are time constants. Therein v_j denotes the valve position deviation from its nominal value for a governor, u_j are the locational marginal prices

(LMPs), and $J_j(\cdot) : \mathbb{R} \to \mathbb{R}$ and $U_j(\cdot) : \mathbb{R} \to \mathbb{R}$ are a generator's cost function and a load's utility function, respectively. We assume $J_j(\cdot)$ is strictly convex while $U_j(\cdot)$ is strictly concave and both are differentiable with derivatives $J_j'(\cdot)$ and $U_j'(\cdot)$, respectively. (2a) and (2b) capture a second-order turbine-governor model for each generator, and (2c) mimics the load dynamics. (2) embodies the rationality of market participants by driving their generations/consumptions to match their marginal cost/utility with LMPs.

2.2 Price Spoofing

The crux of market-based frequency control lies in the design of the price controller $u := (u_j, j \in \mathcal{N})$. The state of the art mainly resorts to model-driven methods to derive state feedback control. For instance, You et al. (2018) proposes a market controller that involves dynamical locational marginal prices (DLMPs), where the controller is designed based on linearized swing dynamics but is resilient to impulse disturbances in the power dynamics.

The performance of the model-driven controller design builds on the premise that a model for the open-loop system (1), (2) is known, accurately parameterized, and well defined. This may not be the case, if the controller was designed assuming a historical or previously calibrated model of the system. Further, market dynamics may be subject to manipulation or vulnerable to cyber-attacks. How vulnerable is a model-driven controller to cyber-attacks or modeling uncertainty?

We consider a simple price spoofing strategy $h(u) = u + \alpha\overline{u}$, where the parameter $\overline{u}$ is unknown. We suppose that $\alpha > 0$ is a constant parameter and $\overline{u}$ is a fixed but unknown price offset imposed by an adversarial agent. The challenge is to simultaneously learn a market controller directly from data, that assumes limited or no *a priori* knowledge of the underlying market and transmission system dynamics, while maintaining robustness to price spoofing.

3. DATA-DRIVEN ONLINE LEARNING OF OPEN-LOOP DYNAMICS

3.1 Input-Koopman Operators

In the presence of unknown price spoofing, any model-driven method to design the controller u is unsatisfactory as it is unable to precisely characterize the open-loop system. This motivates us to develop a data-driven controller robust and adaptive to price spoofing. The key is to learn a representative model of actual system dynamics from limited state data collected in real-time. See Fig. 1 for the new closed-loop system with price spoofing.

Consider (1) and (2) combined with any spoofing strategy as a new hidden open-loop system. We suppose that the spoofing strategy is unknown and that measurements of a subset of system states are made available via SCADA or PMU measurements, in response to current pricing schemes. We use this data to learn the open-loop dynamics via the Koopman operator method proposed by Mezić and Banaszuk (2004); Mezić (2005). The fundamental principle is that the evolution of any set of observables on a dynamical system can be described by the action of

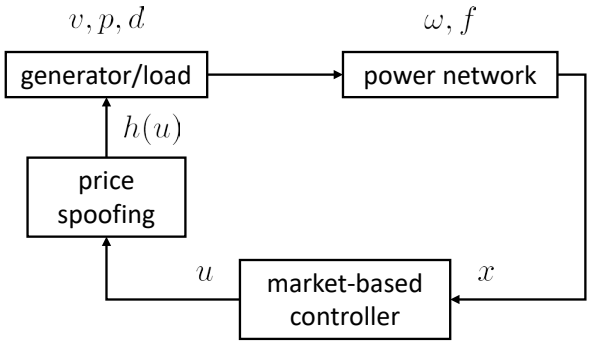

Fig. 1. A schematic of a closed-loop block diagram showing how a data-driven market-based controller interfaces with a transmission power network. The generator frequencies are passed as input data for the market-based controller. A data-driven market-based controller has no *a priori* knowledge of the power network model, but relies on time-series data to generate a control policy for the price signal u. The presence of a spoofing cyber-breach must be learned from the data.

an infinite-dimensional linear operator, i.e., the Koopman operator.

The Koopman operator is powerful in terms of inferring properties of dynamical systems that are either partially or completely unknown. In our system, let $x := \{\omega\} \in \mathbb{R}^{|\mathcal{G}|}$ be the observable states used for calculating the Koopman operator. Line flows f are chosen instead of phase angles θ and voltages E_q' such that all the states x represent deviations from a predetermined static point. We assume without loss of generality that $x^* = \{0, 0, 0, 0, 0\}$ is an equilibrium of economic dispatch.

For simplicity of exposition, we consider a discrete-time treatment, extending the approaches outlined in Mezić and Banaszuk (2004); Susuki and Mezic (2011); Yeung et al. (2017); Proctor et al. (2016). Let x_t be the sampled states at time slot t and u_t be the sampled price controller at time slot t. Then we have:

$$x_{t+1} = g(x_t, u_t) \tag{3}$$

where $g(\cdot) : \mathbb{R}^{|\mathcal{G}|} \times \mathbb{R}^{|\mathcal{N}|} \to \mathbb{R}^{|\mathcal{G}|}$ is a nonlinear function that characterizes the evolution of the swing dynamics Susuki and Mezic (2011).

3.2 Deep Input-Koopman Learning

Proctor et al. (2016); Yeung et al. (2018); Liu et al. (2017) have showed recently that the Koopman operator is generalizable to model the effect of control or input, i.e., the input-Koopman operator, as follows:

$$\psi_x(x_{t+1}) = K_x\psi_x(x_t) + K_u\psi_u(u_t) \tag{4}$$

where $\psi_x(x_t) \in \mathbb{R}^{n_x}, \psi_u(u_t) \in \mathbb{R}^{n_u}$ with $n_x, n_u \leq \infty$ being potentially infinite dimensional dictionaries of observables defined on the state x_t and the input u_t, respectively.

As the input-Koopman model indicates, $\psi_x(x_t)$ and $\psi_u(u_t)$ must belong to lifted spaces in which $\psi_x(x_t)$ evolves according to the linear law (4). Suppose the spans of the dictionary matrices $\mathcal{D}_x := [\psi_x^1(x)\ \psi_x^2(x)\ \dots\ \psi_x^{n_x}(x)]$ and $\mathcal{D}_u := [\psi_u^1(u)\ \psi_u^2(u)\ \dots\ \psi_u^{n_u}(u)]$ cover $\psi_x(x_t)$ and $\psi_u(u_t)$

for all t, respectively. The key to precisely characterizing all nonlinearities is to define comprehensive $\mathcal{D}_x$ and $\mathcal{D}_u$, which however are usually unknown in practice. Instead, the observable state data and input data of dynamical systems are often available and set as a series of points $(x_1, u_1, x_2, u_2, \dots, x_t, u_t, \dots)$, thus whichever functions picked into the dictionaries must satisfy the linear law of (4) with respect to the dataset.

While extended dynamic mode decomposition algorithms Proctor et al. (2016) *a priori*, deep dynamic mode decomposition algorithms Yeung et al. (2017) efficiently generate dictionaries Johnson and Yeung (2018) and traverse function space during training to obtain an accurate estimate of the Koopman operators. In deep input-Koopman learning, a deep neural network that takes x_t or u_t as an input outputs the corresponding dictionary $\psi_x(x_t)$ or $\psi_u(u_t)$. Deep neural networks have rich expressivity with limited layers and thus scale well to large systems Yeung et al. (2017). Finally, with a single training run, they explore thousands to hundreds of thousands of potential dictionary functions in search of a Koopman invariant subspace. This makes deep Koopman operator learning highly effective for applications of data-driven model discovery.

Let $\mathcal{D}_x = \psi_x^{NN}(x_t; \delta_x)$ and $\mathcal{D}_u = \psi_u^{NN}(u_t; \delta_u)$ where $\psi_x^{NN}(x_t; \delta_x)$ and $\psi_u^{NN}(u_t; \delta_u)$ are two neural network (m_x-layer and m_u-layer) with parameters

$$\delta_x = (W_x^1, \dots, W_x^{m_x}, b_x^1, \dots, b_x^{m_x})$$

and respectively for the m_u layer,

$$\delta_u = (W_u^1, \dots, W_u^{m_u}, b_u^1, \dots, b_u^{m_u})$$

. Take $\psi_x^{NN}(x_t; \delta_x)$ as an example,

$$\psi_x^{NN}(x_t; \delta_x) := r^{m_x} \circ r^{m_x - 1} \circ \cdots \circ r^1(x_t) \tag{5}$$

where $r^j(r^{j-1}) := \sigma_x^j(W_x^{j-1} r^{j-1} + b_x^{j-1})$ and $W^{j-1} \in \mathbb{R}^{e^j \times e^{j-1}}$. The number of layers m_x and the number of neurons at each layer e^j are hyper-parameters that are optimized using a combination of dropout and regularization. The activation function $\sigma_x^j(\cdot)$ can be properly chosen for fast convergence, e.g., ELU, cRELU, RELU, etc.

The Koopman operator learning problem is formally formulated as

$$\min_{\substack{K_x, K_u, \\ \delta_x, \delta_u}} ||\psi_x^{NN}(\delta_x; x_{t+1}) - K_x \psi_x^{NN}(\delta_x; x_t) - K_u \psi_u^{NN}(\delta_u; u_t)||_2 \tag{6}$$

Notice that the optimization is with respect to K_x, K_u and all neural network parameters. During deep input-Koopman learning, the dictionaries $\psi_x(x_t), \psi_u(u_t)$ and the Koopman operators K_x, K_u are learned simultaneously. This allows the training algorithm to quickly search over potential representations for Koopman invariant subspaces, as well as the concomitant coordinates for a Koopman operator.

4. ADAPTIVE PRICING CONTROL: KOOPMAN CONTROLLER SYNTHESIS

We now propose a data-driven approach for controller synthesis based on the linear input-Koopman model. Consider the case where the input of the underlying system inherently enters as an additive nonlinearity. The system we consider is of the form:

$$x_{t+1} = g_1(x_t) + g_2(u_t). \tag{7}$$

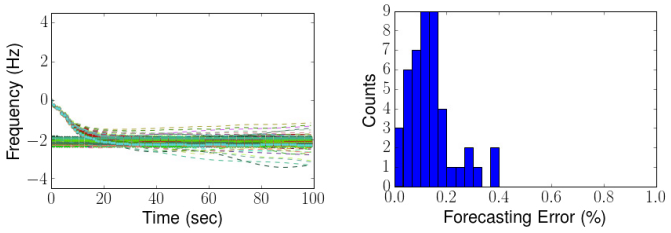

Fig. 2. Evaluation of the deep Koopman learning algorithm, deep dynamic mode decomposition, on 50 simulations of the IEEE 39 bus system subject to spoofing mechanism $h(u)$. Forecasted state trajectories (dashed) vs. ground-truth trajectories (dots) in the test data set (left) and a histogram of the forecasting error across all 50 traces of test data (right). A single initial condition was drawn from the test data set, which the deep Koopman operator propagates forward in 100 time-steps.

When $g_1(x_t) = Ax_t$ is linear, then it suffices to revise the input definition, defining $\bar{u}_t = g_2(u_t)$, and synthesize a stabilizing controller using classical methods. However, we are considering a case where $g_1(x_t)$ is nonlinear and *unknown*, i.e., the swing dynamics and phase differences are written as bilinear or trigonometric terms with unknown parameters or explicit functional form. In Lemma 2 of Liu et al. (2017) we see that the deep Koopman learning problem can be structured to find an input-Koopman operator satisfying

$$\psi_x(x_{t+1}) = K_x \psi_x(x_t) + K_u \psi_u(u_t) \tag{8}$$

Notice that the static feedback control strategy does not result in a tractable linear synthesis problem. Specifically, if we suppose that $u_t = K_c \psi_x(x_t)$, the closed-loop system is then written as

$$\psi_x(x_{t+1}) = K_x \psi_x(x_t) + K_u \psi_u(K_c \psi_x(x_t)) \tag{9}$$

which is nonlinear in $\psi_x(\cdot)$. An alternative is to try and write $\psi_u(u_t) \equiv K_c \psi_x(x_t)$ to solve for a static feedback law K_c, but this is equivalent to assuming that $\psi_u(u_t)$ is within the span of $\psi_x(x_t)$, imposing an unnatural constraint on the learning problem.

Instead, we consider a dynamic feedback approach. Take $\psi_u(u_t)$ as the *output* of a dynamical control system, with internal control state $\psi_\nu(\nu_t)$. We construct $\psi_\nu(\nu_t)$, independent of the learning process for $\psi_x(x_t)$, such that $\psi_u(u_t)$ is in the span of $\psi_\nu(\nu_t)$:

$$\psi_u(u_t) = C_\nu \psi_\nu(\nu_t) \tag{10}$$

We define the dynamical controller equations as

$$\psi_\nu(\nu_{t+1}) = A_\nu \psi_\nu(\nu_t) + B_\nu y_t \tag{11}$$

where $y_t = \psi_x(x_t)$ is the output from the open-loop system or uncontrolled input-Koopman system. We can write the entire closed-loop system in the form:

$$\begin{aligned} \psi_x(x_{t+1}) &= K_x \psi_x(x_t) + K_u \tau_t \\ \psi_\nu(\nu_{t+1}) &= A_\nu \psi_\nu(\nu_t) + B_\nu y_t \\ \tau_t &= \psi_u(u_t) = C_\nu \psi_\nu(\nu_t) \\ y_t &= \psi_x(x_t) \end{aligned} \tag{12}$$

or more compactly,

$$\begin{bmatrix} \psi_x(x_{t+1}) \\ \psi_u(u_{t+1}) \end{bmatrix} = \begin{bmatrix} K_x & K_u C_\nu \\ B_\nu & A_\nu \end{bmatrix} \begin{bmatrix} \psi_x(x_t) \\ \psi_u(u_t) \end{bmatrix} \tag{13}$$

Consider a quadratic Lyapunov function for the above Koopman system of the form

$$\begin{aligned} & V_{\mathcal{L}}(x_{t+1}, u_{t+1}) \\ &= \begin{bmatrix} \psi_x(x_{t+1}) \\ \psi_u(u_{t+1}) \end{bmatrix}^T P_{\mathcal{L}} \begin{bmatrix} \psi_x(x_{t+1}) \\ \psi_u(u_{t+1}) \end{bmatrix} \\ &= \begin{bmatrix} \psi_x(x_t) \\ \psi_u(u_t) \end{bmatrix}^T \begin{bmatrix} K_x & K_u C_\nu \\ B_\nu & A_\nu \end{bmatrix}^T P_{\mathcal{L}} \begin{bmatrix} K_x & K_u C_\nu \\ B_\nu & A_\nu \end{bmatrix} \begin{bmatrix} \psi_x(x_t) \\ \psi_u(u_t) \end{bmatrix} \end{aligned} \tag{14}$$

where $P_{\mathcal{L}} := \begin{bmatrix} P_1 & 0 \\ 0 & P_2 \end{bmatrix} \succ 0$ is of proper dimension. Let $Q := \begin{bmatrix} K_x & K_u C_\nu \\ B_\nu & A_\nu \end{bmatrix}$. Then we have

$$\begin{aligned} & V_{\mathcal{L}}(x_{t+1}, u_{t+1}) < V_{\mathcal{L}}(x_t, u_t) \\ \Leftrightarrow & \begin{bmatrix} \psi_x(x_t) \\ \psi_u(u_t) \end{bmatrix}^T Q^T P_{\mathcal{L}} Q \begin{bmatrix} \psi_x(x_t) \\ \psi_u(u_t) \end{bmatrix} \\ & < \begin{bmatrix} \psi_x(x_t) \\ \psi_u(u_t) \end{bmatrix}^T P_{\mathcal{L}} \begin{bmatrix} \psi_x(x_t) \\ \psi_u(u_t) \end{bmatrix} \end{aligned} \tag{15}$$

i.e.,

$$P_{\mathcal{L}} - Q^T P_{\mathcal{L}} Q \succ 0 \tag{16}$$

Therefore, (16) suffices to guarantee that the closed-loop system (12) is asymptotically stable. By the Schur complement theorem,

$$\begin{aligned} & P_{\mathcal{L}} - Q^T P_{\mathcal{L}} Q \succ 0 \\ \Leftrightarrow & \begin{bmatrix} P_{\mathcal{L}} & Q^T \\ Q & P_{\mathcal{L}}^{-1} \end{bmatrix} \succ 0 \\ \Leftrightarrow & \begin{bmatrix} P_1 & 0 & K_x^T & B_\nu^T \\ 0 & P_2 & C_\nu^T K_u^T & A_\nu^T \\ K_x & K_u C_\nu & P_1^{-1} & 0 \\ B_\nu & A_\nu & 0 & P_2^{-1} \end{bmatrix} \succ 0 \\ \Leftrightarrow & \begin{bmatrix} P_1 & 0 & K_x^T P_1 & B_\nu^T P_2 \\ 0 & P_2 & C_\nu^T K_u^T P_1 & A_\nu^T P_2 \\ P_1 K_x & P_1 K_u C_\nu & P_1 & 0 \\ P_2 B_\nu & P_2 A_\nu & 0 & P_2 \end{bmatrix} \succ 0 \end{aligned} \tag{17}$$

where in the last line we have multiplied by a block matrix to eliminate the inverse terms. We consider a change of variables,

$$P_2 B_\nu = \bar{B}_\nu, P_2 A_\nu = \bar{A}_\nu, P_1 K_u C_\nu = \bar{C}_\nu \tag{18}$$

Since the above constraint is a linear matrix inequality (LMI) in the variables $(P_1, P_2, \bar{A}_\nu, \bar{B}_\nu, \bar{C}_\nu)$, the problem is a convex semidefinite program (SDP). We can solve for $(P_1, P_2, \bar{A}_\nu, \bar{B}_\nu, \bar{C}_\nu)$ first and then recover the controller (A_ν, B_ν, C_ν) by

$$A_\nu = \bar{A}_\nu P_2^{-1}, \quad B_\nu = \bar{B}_\nu P_2^{-1}, \tag{19}$$

Under this change of variables, if the LMI constraint is satisfied, the closed-loop system (12) asymptotically converges to the original equilibrium point of economic dispatch x^*, where the nominal frequency is restored and economic efficiency is recovered.

Note that the solution to this problem is for a linear control problem, since it leverages the linear form of a Koopman operator and a closed-loop Koopman dynamical system. However, the true control law learned by the Koopman operator is nonlinear in $x(t)$, since it is a function of the nonlinear mapping $\psi_x(x_t)$. We can write the discrete control law as

$$\psi_u(u_t) = C_\nu A_\nu^t \tau_0 + \sum_{k=0}^{t} A_\nu^{t-1-k} B_\nu \psi_x(x_k) \tag{20}$$

We have thus derived an approach for discovering nonlinear control laws on systems that satisfy the input-state separability properties of Lemma 2 in Liu et al. (2017). Our future work will investigate closed-loop controller synthesis using the Koopman approach for arbitrary nonlinear systems.

5. DEEP KOOPMAN CONTROLLER SYNTHESIS: SIMULATION EXAMPLE ON A COMPROMISED IEEE 39 BUS SYSTEM

Next we tested our deep Koopman controller synthesis approach on the IEEE 39-bus benchmark system with initial set points from the power system toolbox (PST). To mimic the online setting where the state data and input data of the dynamical system are available, we manually generate a dataset of the open-loop system with linear but unknown price spoofing $h(u) = u + \alpha\bar{u}$, where $\alpha = 1$ and $\bar{u} = 8$. We suppose the model for the system is unknown or subject to modeling uncertainty. Moreover, we suppose that only time-series data of the generator frequencies are available for SCADA monitoring (ω trajectories). All other states in the system model (1a)-(1d) are assumed to be unmeasured.

Our dataset thus consists of 100 simulated ω time-series trajectories of a 40 second system evolution (500 data points). We trained and evaluated a deep Koopman operator using a randomized 50%/50% training-test data split.

We immediately observed that in the absence of a stabilizing market controller, the power system was unable to converge to the desired frequency of 60 Hz. The network consistently converged to a lower frequency of 58 Hz, outside the permitted operational limits of the power system.

Our deep Koopman operator demonstrated excellent 1-step ($< 0.01\%$ test error) and 100-step prediction accuracy ($< 10\%$ test error) on the test data (see Figure 2. Remarkably, the deep Koopman operator was able to predict across 50 distinct initial conditions in the phase space of the power system model, indicating strong generalization and bias-variance tradeoffs. We also noted divergence of forecasted trajectories after 60 steps, though the majority of traces maintained stability or evolved with a qualitatively similar shape as the ground-truth trajectories. We also computed the controllability matrix of the learned Koopman representation, using the system matrices (K_x, K_u) and found that the system was indeed controllable.

For the controller synthesis step, we first transformed the learned Koopman system from a discrete state-space model to a continuous model using the Tustin transformation. This made it possible to directly integrate Python simulations of the system model (1a)-(1d) with the closed-loop controller model. We considered two approaches to synthesizing a controller, first the LMI constrained method described in the previous section to design a dynamical model of a controller and second, using a continuous algebraic Ricatti equation approach. Both strategies result in a dynamic pricing policy, where the price $p_j(t)$ in equation

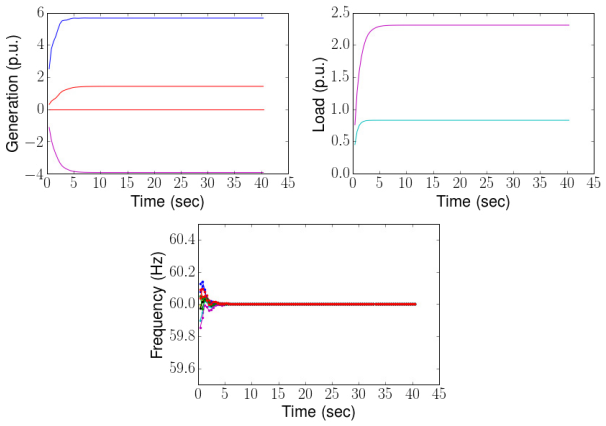

Fig. 3. Closed-loop dynamics of the transmission system with a deep Koopman controller deciding price signals as a function of all generator frequencies.

(2a)-(2c) is now dependent on time and the data-driven controller synthesized from the corresponding design algorithm. Despite absence of specific knowledge of the system model and the presence (and parameters) of a spoofing offset, the deep Koopman controller is able to stabilize the system to a steady-state frequency of 60 Hz, plus or minus 0.01 Hz, in less than 5 seconds time. The temporary swing transients do not exceed 0.2 Hz on either side of the 60 Hz setpoint. Thus, we are able to perform secondary frequency control using only frequency time-series measurements.

6. CONCLUSION

In this paper we developed a data-driven controller synthesis algorithm using deep input-Koopman operators for market-based frequency regulation in the presence of price spoofing. Deep neural networks are used to learn an input-Koopman operator model of the open-loop system dynamics in the presence of price spoofing. We derive an equivalent H2 synthesis algorithm as a semi-definite program and we show the proposed method is able to offset price spoofing by restoring the nominal frequency and recovering economic efficiency on the IEEE 39 benchmark system. Future research will investigated design of distributed data-driven control architectures, leveraging advances in Koopman decomposition Liu et al. (2017) and Koopman control Williams et al. (2016); Yeung et al. (2018).

REFERENCES

Alvarado, F.L., Meng, J., DeMarco, C.L., and Mota, W.S. (2001). Stability analysis of interconnected power systems coupled with market dynamics. *IEEE Transactions on power systems*, 16(4), 695–701.

Johnson, C.A. and Yeung, E. (2018). A class of logistic functions for approximating state-inclusive koopman operators. *Proceedings of the 2018 IEEE American Control Conference*.

Jokic, A., Van Den Bosch, P., and Hermans, R. (2009). Distributed, price-based control approach to market-based operation of future power systems. In *Energy Market, 2009. EEM 2009. 6th International Conference on the European*, 1–6. IEEE.

Li, N., Zhao, C., and Chen, L. (2016). Connecting automatic generation control and economic dispatch from an optimization view. *IEEE Transactions on Control of Network Systems*, 3(3), 254–264.

Liang, Y., Liu, F., and Mei, S. (2015). Stability analysis of the hybrid dynamics coupling power systems with power markets. In *Power & Energy Society General Meeting, 2015 IEEE*, 1–5. IEEE.

Liu, Z., Kundu, S., Chen, L., and Yeung, E. (2017). Decomposition of nonlinear dynamical systems using koopman gramians. *arXiv preprint arXiv:1710.01719*.

Mallada, E., Zhao, C., and Low, S. (2017). Optimal load-side control for frequency regulation in smart grids. *IEEE Transactions on Automatic Control*, 62(12), 6294–6309.

Mezić, I. (2005). Spectral properties of dynamical systems, model reduction and decompositions. *Nonlinear Dynamics*, 41(1-3), 309–325.

Mezić, I. and Banaszuk, A. (2004). Comparison of systems with complex behavior. *Physica D: Nonlinear Phenomena*, 197(1-2), 101–133.

Pang, J.Z., Guo, L., and Low, S.H. (2017). Load-side frequency regulation with limited control coverage. *SIGMETRICS Perform. Eval. Rev.*, 45(2), 94–96.

Proctor, J.L., Brunton, S.L., and Kutz, J.N. (2016). Dynamic mode decomposition with control. *SIAM Journal on Applied Dynamical Systems*, 15(1), 142–161.

Stegink, T., De Persis, C., and van der Schaft, A. (2017). A unifying energy-based approach to stability of power grids with market dynamics. *IEEE Transactions on Automatic Control*, 62(6), 2612–2622.

Stegink, T.W., De Persis, C., and van der Schaft, A.J. (2016). Stabilization of structure-preserving power networks with market dynamics. *arXiv preprint arXiv:1611.04755*.

Susuki, Y. and Mezic, I. (2011). Nonlinear koopman modes and coherency identification of coupled swing dynamics. *IEEE Transactions on Power Systems*, 26(4), 1894–1904.

Wang, Z., Liu, F., Pang, J.Z., Low, S., and Mei, S. (2017). Distributed optimal frequency control considering a nonlinear network-preserving model. *arXiv preprint arXiv:1709.01543*.

Williams, M.O., Hemati, M.S., Dawson, S.T., Kevrekidis, I.G., and Rowley, C.W. (2016). Extending data-driven koopman analysis to actuated systems. *IFAC-PapersOnLine*, 49(18), 704–709.

Yeung, E., Kundu, S., and Hodas, N. (2017). Learning deep neural network representations for koopman operators of nonlinear dynamical systems. *arXiv preprint arXiv:1708.06850*.

Yeung, E., Liu, Z., and Hodas, N.O. (2018). A koopman operator approach for computing and balancing gramians for discrete time nonlinear systems. *Proceedings of the 2018 IEEE American Control Conference*.

You, P., Pang, J.Z., and Yeung, E. (2018). Stabilization of power networks via market dynamics. *Technical report*.

Zhao, C., Mallada, E., Low, S., and Bialek, J. (2016). A unified framework for frequency control and congestion management. In *Power Systems Computation Conference (PSCC), 2016*, 1–7. IEEE.

Zhao, C., Topcu, U., Li, N., and Low, S. (2014). Design and stability of load-side primary frequency control in power systems. *IEEE Transactions on Automatic Control*, 59(5), 1177–1189.